Acta Neurochirurgica (2019) 161:2453–2466
https://doi.org/10.1007/s00701-019-04052-7

ORIGINAL ARTICLE - PERIPHERAL NERVES

# Pathologic remodeling in human neuromas: insights from clinical specimens

Mark A. Mahan[1] · Hussam Abou-Al-Shaar[2] · Michael Karsy[1] · Wesley Warner[1] · Stewart Yeoh[1] · Cheryl A. Palmer[3]

Received: 28 February 2019 / Accepted: 22 August 2019 / Published online: 14 October 2019


## Abstract

**Background** Neuroma pathology is commonly described as lacking a clear internal structure, but we observed evidence that there are consistent architectural elements. Using human neuroma samples, we sought to identify molecular features that characterize neuroma pathophysiology.

**Methods** Thirty specimens—12 neuromas-in-continuity (NICs), 11 stump neuromas, two brachial plexus avulsions, and five controls—were immunohistochemically analyzed with antibodies against various components of normal nerve substructures.

**Results** There were no substantial histopathologic differences between stump neuromas and NICs, except that NICs had intact fascicle(s) in the specimen. These intact fascicles showed evidence of injury and fibrosis. On immunohistochemical analysis of the neuromas, laminin demonstrated a consistent double-lumen configuration. The outer lumen stained with GLUT1 antibodies, consistent with perineurium and microfascicle formation. Antibodies to NF200 revealed small clusters of small-diameter axons within the inner lumen, and the anti-S100 antibody showed a relatively regular pattern of non-myelinating Schwann cells. CD68+ cells were only seen in a limited temporal window after injury. T-cells were seen in neuroma specimens, with both a temporal evolution as well as persistence long after injury. Avulsion injury specimens had similar architecture to control nerves. Seven pediatric specimens were not qualitatively different from adult specimens. NICs demonstrated intact but abnormal fascicles that may account for the neurologically impoverished outcomes from untreated NICs.

**Conclusions** We propose that there is consistent pathophysiologic remodeling after fascicle disruption. Particular features, such as predominance of small caliber axons and persistence of numerous T-cells long after injury, suggest a potential role in chronic pain associated with neuromas.

**Keywords** Endoneurial tubule · Extracellular matrix · Laminin · Perineurium · Peripheral nerve injury · Schwann cell

## Introduction

The conceptualization of a regenerative neuroma has a long history [30] with significant controversy. Wood [51] ascribed the word "neuroma" to Odier in 1811 [37] in describing these lesions, believing that the proliferation at the end of a nerve was a tumor, which was a common opinion for at least a hundred years [32]. This regenerative quality of a neuroma was explored in greater detail by Cajal [41], who traced axons using silver stains. He carefully depicted axonal sprouting through the use of ingenious models of transection to demonstrate the capacity as well as frustrations of axons to re-establish connection to a distal nerve—promoting the concept of purposeful nerve regeneration. However, a more recent and dominant view is that expressed by Sunderland, who described neuromas as pathologically "disorganized" structures that "aggravate the axonal loss and erroneous cross-shunting"

This article is part of the Topical Collection on *Peripheral Nerves*

**Electronic supplementary material** The online version of this article (https://doi.org/10.1007/s00701-019-04052-7) contains supplementary material, which is available to authorized users.

✉ Mark A. Mahan
mark.mahan@hsc.utah.edu

[1] Department of Neurosurgery, Clinical Neurosciences Center, University of Utah, 175 North Medical Drive East, Salt Lake City, UT 84132, USA

[2] Department of Neurological Surgery, University of Pittsburgh Medical Center, Pittsburgh, PA, USA

[3] Department of Pathology, University of Utah, Salt Lake City, UT, USA

[45]. This conceptualization of neuromas as chaotic masses continues; it is currently conceived as a molecular cascade resulting from deposition of fibrin within the nerve that leads to a fibrous, disorganized mass of fibroblasts and macrophages, among other cellular elements [7]. Thus, there is a duality of perspective on the profound cellular expansion after nerve injury: the regenerative capacity to re-establish innervation compared with the hopeless and chaotic scar.

We recently noted that neuromas, whether in-continuity or transection (stump) injuries, demonstrate a conserved feature of extracellular protein remodeling [22]. We sought to explore and delineate the microarchitecture of neuromas with additional immunohistochemical (IHC) evaluation to assess for consistent patterns within neuromas and to better understand the pathophysiology of these lesions.

## Materials and methods

The study was approved by the institutional review board at the University of Utah with wavier of informed consent from the patients involved in the study. All patients of the lead author (MAM) who underwent surgical resection of neuromas as part of their surgical treatment between October 2016 and June 2017 had specimens sent for pathological and IHC evaluation. No patient with sufficient nerve tissue available for evaluation was excluded. These specimens were then categorized into three study groups: the stump neuroma group, the neuroma-in-continuity (NIC) group, and the avulsion group. Control specimens were obtained during neurectomy surgery for spasticity reduction arising from stroke from April to June 2017 and compared with the study groups. No control specimens were excluded.

Histological analysis of tissue samples was performed at the direction of the senior author and neuropathologist (CAP), and the methods have been previously reported [22]. Briefly, histologic studies included hematoxylin and eosin (H&E) and trichrome stains. Additional clinically available immunohistochemical (IHC) markers, namely, laminin (Novus Biologicals, Centennial, CO, USA, 1:100 dilution), GLUT1 (Abcam, Cambridge, United Kingdom, 1:600 dilution), NF200 (Dako Agilent, Santa Clara, CA, USA, 1:400 dilution), S100 (Dako, 1:5000 dilution), and CD68 (Dako, 1:6000 dilution), CD25 (Leica Biosystems, Buffalo Grove, IL, USA, mouse clone 4C9), CD3 (Ventana Medical Systems/Roche, Tucson, AZ, USA, rabbit clone 2GV6), and CD4 (Ventana, rabbit clone SP35), were used to depict endoneurial extracellular matrix, perineurial, axonal, Schwann cell, activated macrophages, regulatory T-cells, total T-cells, and helper T-cells, respectively.

Five-micrometer, formalin-fixed, paraffin-embedded sections of neuroma resections from all patients were cut at regular intervals and mounted on glass sides. H&E, trichrome, and IHC stains were prepared on all specimens. Immunohistochemical staining was performed using commercial antibodies at the manufacturers' recommended dilutions. Staining was performed using the avidin-biotinylated peroxidase complex (ABC) method on a Ventana Staining system and counterstained with hematoxylin. Chromogenic multiplex immunohistochemical staining was performed on the BenchMark Discovery staining system (Ventana) using a sequential application of three primary antibodies (panel of NF200, CD68, and S100 and a panel of CD25, CD3, and CD4) with a heat activation step between staining cycles to remove unbound reagent. The Discovery horseradish peroxidase (Purple and Teal) and alkaline phosphatase (Yellow) detection kits use hapten-linked multimer technology and were used to identify the antibody targets (NF200: teal; CD68: purple; S100: yellow; CD25: purple, CD3: yellow, CD4: teal).

Patients' demographics, neuroma classification, time from injury, Sunderland classification of injury, and descriptive histopathological and IHC findings were recorded and analyzed. Axon diameter analysis was performed on NIC specimens at × 400 magnification and control specimens at × 200. Images were converted to grayscale and subjected to local thresholding (Phansalkar's method) using ImageJ (NIH, Bethesda, MD) to identify axons. Particles were then filtered for size (10–10,000 pixels, corresponding to 0.6- to 19.5-μm diameter) and circularity ($= 4\pi \times \text{area/perimeter}^2$), range 0.40–1.00). Statistical analysis was performed using the Kolmogorov–Smirnov test on the continuous distribution as well as Pearson's chi-squared test for binned analysis. $p$ Values less than 0.05 were considered statistically significant.

## Results

Thirty patients were included in the analysis. The summary of all 30 patients is shown in Table 1. The stump group included 11 patients with neuromas without physical connection to a distal nerve; the NIC group included 12 patients with a non-functioning or minimally functioning nerve (no nerve action potential recorded intraoperatively) with the appearance of a NIC (Sunderland grade 4); the avulsion group included two patients with traumatic brachial plexus avulsion injuries; and the control group included five patients who had uninjured, non-pathologic nerve removed for reduction of focal spasticity. Four of the specimens from the NIC group were from surgical nerve grafting for neonatal brachial plexus palsy.

There were 21 male and nine female patients, with a mean age of 34.3 ± 20.9 years (95% confidence interval) including seven total pediatric patients. The mean time from injury to surgical intervention was 24.7 months among all groups (2 days–120 months). The wide range of surgical dates is due to mixture of some patients undergoing nerve repair in the acute or subacute period after injury whereas others undergoing neuroma resection for amelioration of chronic pain

**Table 1** Patients' demographics and etiology characteristics

| Patient | Age | Sex | Etiology | Time from injury | Sunderland classification |
|---|---|---|---|---|---|
| 1 | 60 years | M | Stump neuroma | 120 months | 5 |
| 2 | 58 years | F | Stump neuroma | 60 months | 5 |
| 3 | 50 years | M | Stump neuroma | 10 months | 5 |
| 4 | 64 years | F | Stump neuroma | 48 months | 5 |
| 5 | 26 years | F | Stump neuroma | 12 months | 5 |
| 6 | 17 years | F | Stump neuroma | 13 days | 5 |
| 7 | 58 years | M | Stump neuroma | 6 days | 5 |
| 8 | 49 years | M | Stump neuroma | 24 months | 5 |
| 9 | 41 years | M | Stump neuroma | 17 months | 5 |
| 10 | 61 years | M | Stump neuroma | 18 months | 5 |
| 11 | 26 years | M | Stump neuroma | 3 months | 5 |
| 12 | 6 months | M | NIC | 6 months | 4 |
| 13 | 6 months | F | NIC | 6 months | 4 |
| 14 | 3 months | F | NIC | 3 months | 4 |
| 15 | 37 years | M | NIC | 10 months | 4 |
| 16 | 55 years | M | NIC | 9 months | 4 |
| 17 | 27 years | M | NIC | 11 months | 4 |
| 18 | 31 years | M | NIC | 17 months | 4 |
| 19 | 4 months | M | NIC | 4 months | 4 |
| 20 | 26 years | F | NIC | 12 months | 4 |
| 21 | 13 years | F | NIC | 3 months | 4 |
| 22 | 21 months | F | NIC | 5 months | 4 |
| 23 | 40 years | M | NIC | 18 months | 4 |
| 24 | 25 years | M | Avulsion | 2 days | NA |
| 25 | 27 years | M | Avulsion | 5 months | NA |
| 26 | 51 years | M | Normal nerve | 48 months | NA |
| 27 | 51 years | M | Normal nerve | 60 months | NA |
| 28 | 63 years | M | Normal nerve | 120 months | NA |
| 29 | 40 years | M | Normal nerve | 72 months | NA |
| 30 | 31 years | M | Normal nerve | 18 months | NA |

*NIC* neuroma-in-continuity, *NA* not applicable

after nerve injury. Photomicrographs of each stain for each specimen are included in the Supplemental Fig. 1.

## Cellular and nerve architecture: H&E and trichrome stains

In the stump and NIC groups, H&E and trichrome demonstrated similar hypercellular whorls around axons (Fig. 1a–d), except for three specimens (see below). Substantial deposition of extracellular collagen surrounded clumps of cells (Fig. 1a, b), and there were numerous capillaries in the collagenous stroma. The NIC group was hallmarked by the presence of an intact fascicle in almost all samples. Intact fascicles were also occasionally found in neuromas of the stump group. However, the intact fascicles were not normal (Fig. 1c). All fascicles in the injured nerves had notably hypercellular endoneurium; these cells had tapered nuclei and were not of apparent hematopoietic lineage. These intact fascicles were edematous with myxoid degeneration. The outer layer of the intact fascicle demonstrated thickening of the perineurium.

The avulsion group did not demonstrate this hypercellularity and appeared more similar to the control group. However, one avulsion specimen, from a patient 5 months from injury, demonstrated hypercellularity of the connective tissue external to the nerve.

Three acute specimens, two from the stump group and one from the avulsion group, demonstrated minimal architectural change from control specimens, except for increased cellularity (Fig. 1d, e) in the two stump specimens. These three specimens had the shortest times since injury, ranging from 2 to 13 days after injury, whereas other specimens were all ≥ 3 months after injury. This indicates that neuroma formation is a subacute to chronic process, dependent upon regeneration or remodeling.

## Endoneurial extracellular matrix: laminin

Laminin is an extracellular basement membrane protein produced by Schwann cells and forms the guidance channel for regenerating axons [8]. Laminin IHC showed aberrant extracellular matrix (ECM) formation, with uneven and abnormal "double-lumen" endoneurial tubes in both the stump and NIC groups (Fig. 2a–d). The laminin IHC of the neuromatous sections of the NIC group (Fig. 2a) were indistinguishable from the neuroma of the stump group (Fig. 2b). In contrast, the avulsion group demonstrated laminar-parallel extracellular protein deposition with minimal disruption (Fig. 2c), similar to the control group, which demonstrated intact ECM formation and normal laminin IHC staining (Fig. 2d), consistent with lack of ECM remodeling in avulsion specimens, in comparison with neuroma specimens.

## Axon: NF200

Neurofilaments are cytoskeletal proteins of axons, and NF200 is a marker for mature axonal processes, principally in larger myelinated fibers [43]. Among patients with neuromas (NIC and stump groups), NF200 IHC staining showed small clusters of axons within the inner lumen of the laminin double lumen, consistent with microfascicle formation (Fig. 3a). Thus, the axons of the neuroma are contained in organized bundles within the thick collagenous stroma of the neuroma. There was a conspicuous absence of large-diameter axons in neuroma tissue; therefore, we compared automated image analysis of axon diameters between NIC and control specimens (Fig. 3b). Statistical analysis of the continuous distribution of axon diameters as well as binned analysis of axon diameters (small axons 0.5 μm to < 1.5 μm; intermediate axons 1.5 μm to < 2.5 μm; large axons ≥ 2.5 μm) demonstrated substantial statistical difference between the neuroma and control specimens ($p < 0.00001$, Kolmogorov–Smirnov and Pearson's chi-squared tests, respectively). Approximately 5% of measured axons were ≥ 2.5 μm in neuroma specimens, as compared with 31% in control specimens (Fig. 3c).

The arrangement of NF200 staining in the specimens of the avulsion group was similar to that of control specimens, with undulating fibers in a dense array, because of the persistence of viable sensory fibers from the intact dorsal root ganglion. However, the acute avulsion (2 days after injury) specimen demonstrated much denser NF200 IHC staining (Fig. 3d), as compared with the chronic (5 months after injury) specimen (Fig. 3e), presumably because of the absence of Wallerian degeneration of motor fibers from the spinal cord.

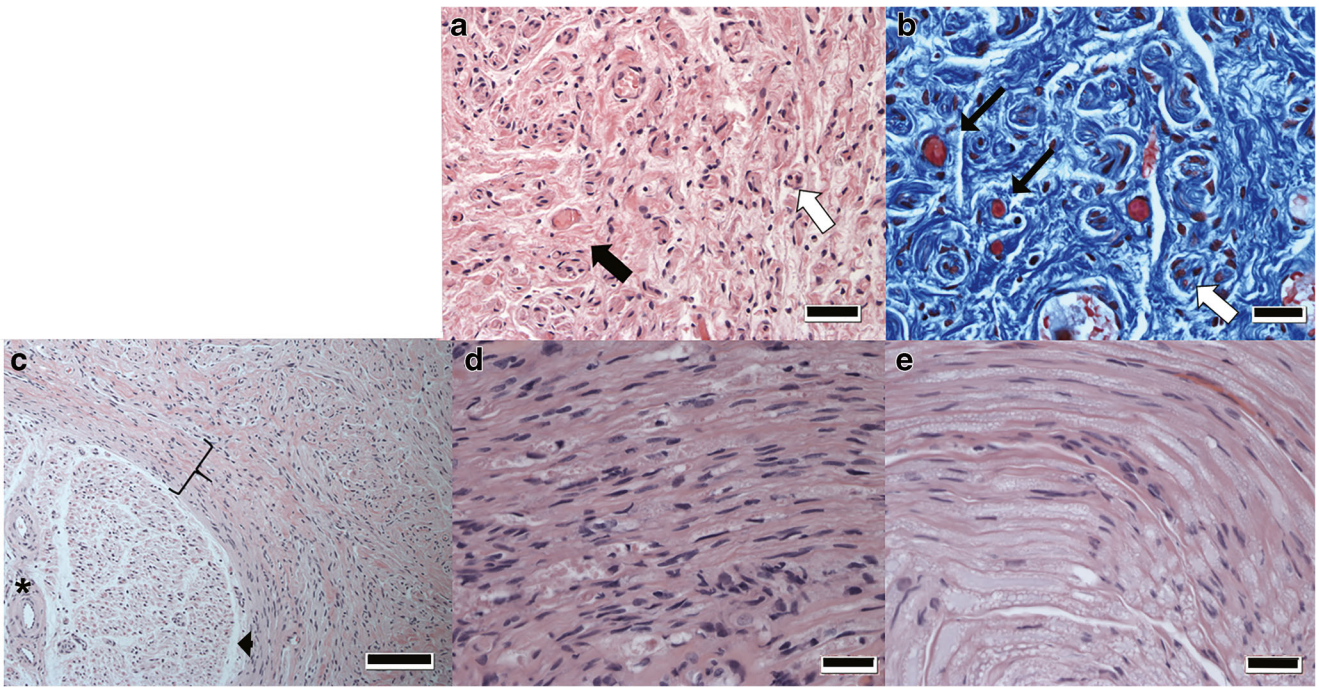


**Fig. 1** H&E and trichrome stains used for delineating structural morphology and collagen deposition. **a** Hypercellular whorls can be seen around axonal clearings (open arrow), embedded in a collagenous matrix (black arrow) (× 400; bar= 20 μm). **b** Trichrome stains also identify the hypercellular bundles as distinct from the collagenous stroma (open arrow) and recognize numerous capillaries (thin black arrows) interspersed in the connective tissue (× 400; bar= 20 μm). **c** Intact fascicles were nearly universally identified in all NIC specimens (arrowhead), surrounded by neuromatous, hypercellular tissue. The intact fascicles were different than control specimens with a thickened perineurial rind (bracket), perivascular thickening (asterisk), and endoneurial hypercellularity (× 100; bar= 100 μm). **d**, **e** An intact fascicle within a stump specimen at 13 days after injury (**d**, × 800; bar= 10 μm) was more cellular than control specimens (**e**, × 800; bar= 10 μm)

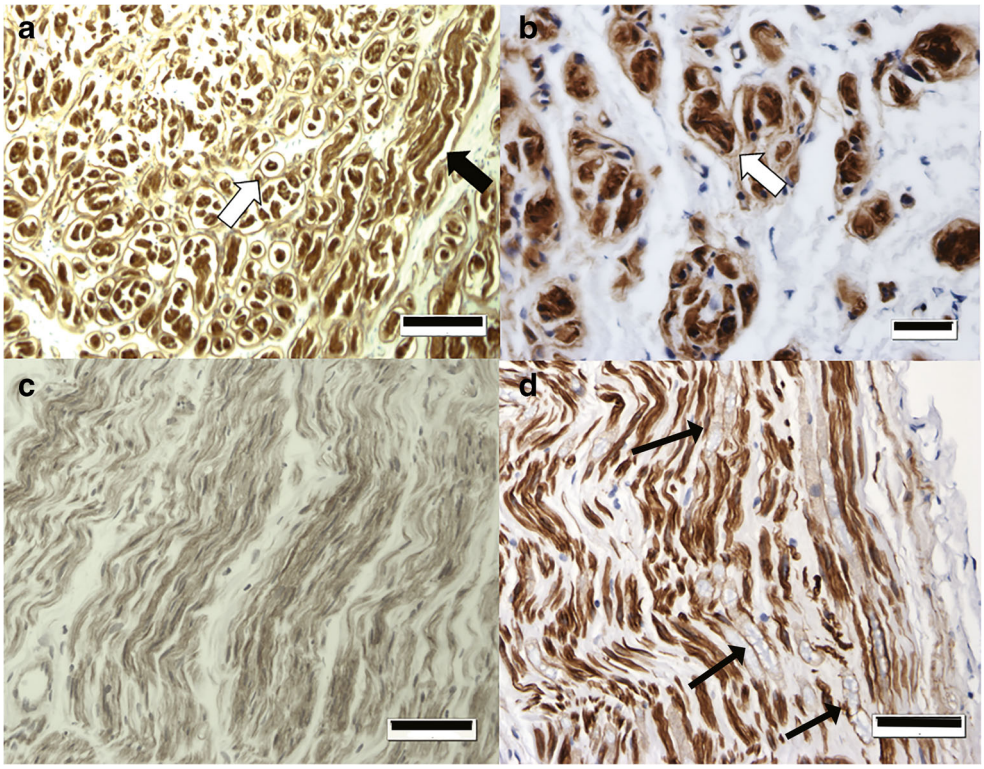


**Fig. 2** Laminin IHC stains. Laminin is a key component of the nerve endoneurial ECM, which forms the guidance channels following nerve injury and regeneration. **a**, **b** Uneven and abnormal "double-lumen" endoneurial tubes are seen in both the stump (**a**, × 100; bar= 100 μm) and NIC groups (**b**, × 400; bar= 20 μm). The open arrow depicts on-end axial slicing of the double-lumen channel; longitudinal slicing of the double-lumen is marked with solid black arrow. **c**, **d** In contrast, there was no evidence of ECM remodeling in avulsion specimens (**c**, × 200; bar= 50 μm) as compared with control specimens (**d**, × 200; bar= 50 μm). Both control and avulsion specimens demonstrate normal undulation of the ECM with laminin IHC outlining Schwann cells (thin black arrows)

## Perineurium: GLUT1

GLUT1 is a known marker of "blood–nerve barrier," avidly demarcating the perineurium in normal nerve tissue [16, 40, 42, 48]. GLUT1 IHC staining was found to correlate with the outer ring of the identified laminin "double lumens" in the NIC and stump groups, identifying these bundles as microfascicles with a perineurial layer (Fig. 4a). The intact fascicles of the NIC and stump groups demonstrated perineurial GLUT1 IHC staining (Fig. 4b) that was thicker than in control specimens, similar to the appearance in H&E (Fig. 1c). The avulsion group (Fig. 4c) had similar GLUT1 IHC staining to control samples.

## Schwann cell: S100

S100 protein is normally present in cells derived from the neural crest, including Schwann cells. S100 staining indicates the presence of phenotypically mature Schwann cells [24]. S100 staining was avid in all neuromas (stump and NIC groups), but only within the microfascicles (Fig. 5a). Interestingly, the S100-positive Schwann cells in the neuroma specimens did not encircle axons, as they do in control specimens (Fig. 5b). In the neuromatous tissue, the S100-positive cells appeared similar to non-myelinating or Remak bundle cells. The only specimen to demonstrate significantly reduced S100 IHC staining, compared with controls, was the chronic avulsion specimen (Fig. 5c). Frequently, S100-positive nerve fibers were seen to be encircling intact fascicles (Fig. 5d), as if they possessed some tropism towards the intact fascicle (Fig. 5d).

## Macrophages: CD68

CD68 is a lysosomal protein expressed in cells of the monocyte lineage, including activated macrophages [18]. Only one specimen had significantly increased CD68 IHC staining, which was a specimen from a full-thickness nerve laceration repaired at 6 days after injury (Fig. 6a). Interestingly, the density of CD68 IHC staining was similar to that seen with brain tissue of a similar-aged cerebral infarct (CAP, personal observation). Many of the CD68-positive cells had long, tapered processes, rather than classic dendritic morphology. The other acute specimens (a stump specimen at 13 days and an avulsion specimen at 2 days after injury, Fig. 6b) demonstrated only mild increase in CD68 staining as compared with chronic neuroma specimens (Fig. 6c). This suggests either a relatively narrow temporal window for activated macrophages or a narrow segment for activated macrophages that may be missed in specimen sampling.

## Triple stain of CD68, NF200, and S100

Triple staining was used to simultaneously evaluate three cells: macrophages (CD68), axons (NF200), and Schwann cells (S100). Staining of control specimens depicted large-

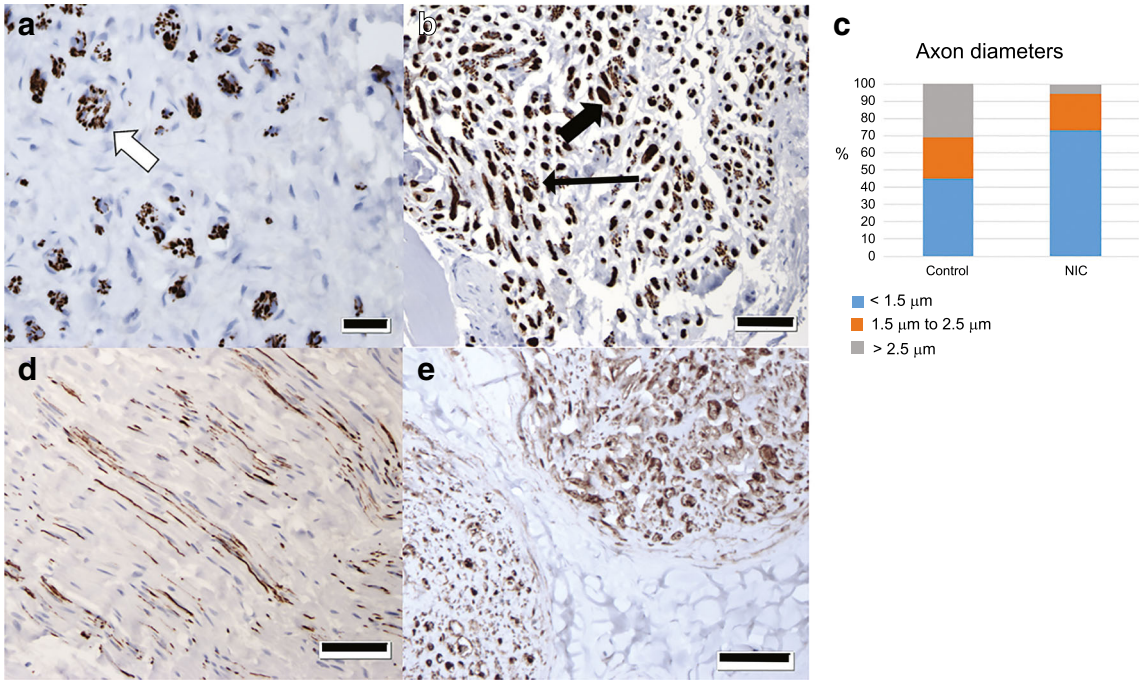


**Fig. 3** Neurofilament (NF200) IHC stains. Neurofilaments are the structural components of axonal processes, and NF200 is a marker for mature axons. **a**, **b** Neuroma specimens (**a**, × 400; bar= 20 μm) demonstrate the presence of bundles of small-diameter fibers (open arrow) admixed within connective tissue stroma of the neuroma, as compared with the normal dense arrays of large fibers (black arrow) and occasional Remak bundles (thin black arrow) of control specimens (**b**, × 200; bar= 50 μm). **c** Axonal diameter measurements displayed as a percentage of total axon counts. **d**, **e** Avulsion specimens demonstrated persistence but substantial reduction in the number of axons at 5 months after injury (**d**, × 200; bar= 50 μm) as compared with essentially normal concentration of axons in a specimen obtained 2 days after injury (**e**, × 200; bar= 50 μm)

diameter axons with typical myelination patterns (Fig. 7a). Acute traumatic laceration at 6 days after injury depicted numerous lipid-filled lysosomes, the majority of which were CD68 positive, although many were not (Fig. 7b). Additionally, not all macrophages were large, potentially different subtypes or activity. Neurofilament was rare and predominantly collected in apparent degradation chambers. Chronic stump neuromas demonstrated abundant S100 in the microfascicles, clustered around occasional neurofilament and without myelination patterns (Fig. 7c). An intact fascicle in a 3-month NIC demonstrates substantially reduced neurofilament with both myelinating and non-myelination S100 morphology (Fig. 7d). Axons with stippled S100 surround the fascicle in a whirled pattern. Infrequent compact CD68 positive cells are seen.

### T-cell markers

Triple staining was also used to evaluate for the T-cell markers CD3 (total T-cells), CD4 (helper T-cells), and CD25 (regulatory T-cells). Recent neuroma specimens (Fig. 8a) demonstrated occasional clusters of T-cells, frequently in association with vascular lumen (Fig. 8b), but not all vascular channels had T-cell clusters (gray arrow, Fig. 8a). Chronic neuroma specimens did not have clusters of T-cells but showed substantial concentrations of T-cells in the stroma of the neuroma (Fig. 8c) in contrast to control specimens (Fig. 8d).

## Discussion

We present IHC evidence of consistent pathologic findings in neuroma specimens, whether from an in-continuity lesion or from a transection injury, that is different from control specimens and avulsion injuries. Five key histologic characteristics have not previously been reported: (1) GLUT1 characterization of microfascicles, (2) the finding of intact fascicles in virtually all NIC specimens, (3) axon diameter measurements in neuroma tissue, (4) patterns of macrophages within neuromas of different ages and types, and (5) appearance of T-cells in human neuromas.

While neuromatous tissue appears chaotic, there are several patterns (Fig. 9). Neuromas only form in a regenerative process that involves fascicle or nerve disruption; they are not present in avulsion or specimens studied less than 3 months after injury. Laminin ECM is remodeled around regenerating axons that traverse the neural scar. Small-diameter axons are clustered into variable-diameter

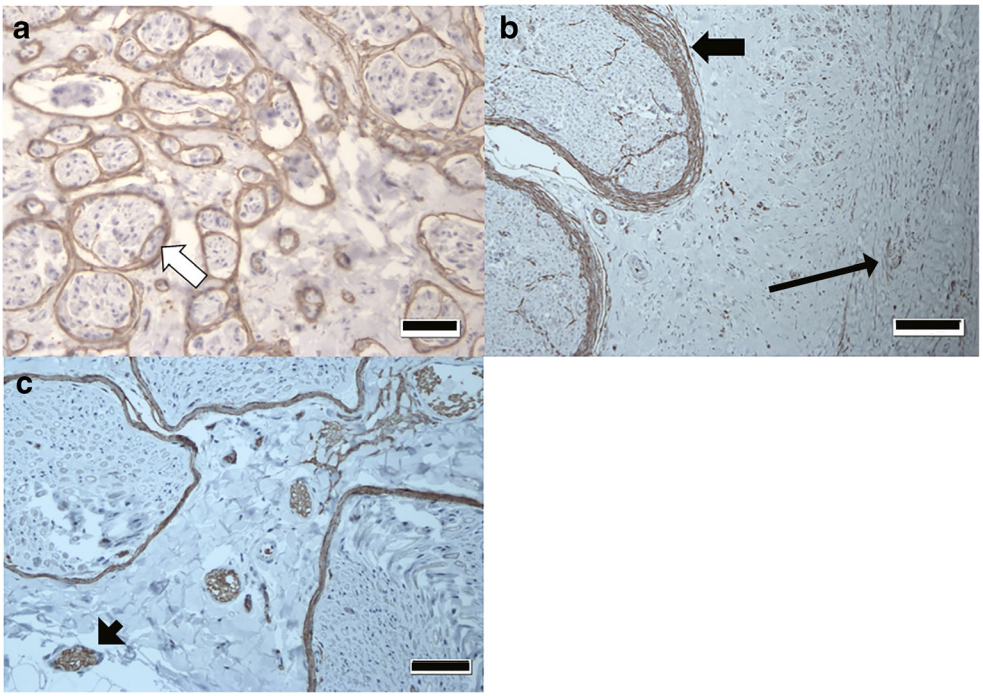


**Fig. 4** GLUT1 IHC stains. GLUT1 is a membrane glucose transporter that is enriched in blood vessels and perineurium and serves as a molecular hallmark of the "blood–nerve barrier." **a** GLUT1 is dense around the outer layer of the double-lumen (open arrow) seen in the laminin IHC stained samples (cf. Fig. 2b), with identical appearance in stump and NIC (× 400; bar= 20 μm) specimens, indicative of microfascicle formation in the neuromatous tissue. **b** Intact fascicles in the neuroma specimens (× 100; bar= 100 μm) demonstrate thickening of the perineurium (black arrow) with 6–10 cellular layers, as was seen in H&E (cf. Fig. 1c), and GLUT1-outlined microfascicles (thin black arrow) of the neuromatous tissue. **c** Avulsion specimens demonstrated GLUT1 staining with normal perineurial thickness (× 200; bar= 50 μm) with 3–4 cellular layers. GLUT1 also stains erythrocytes, seen in the vessel lumens (arrowhead)

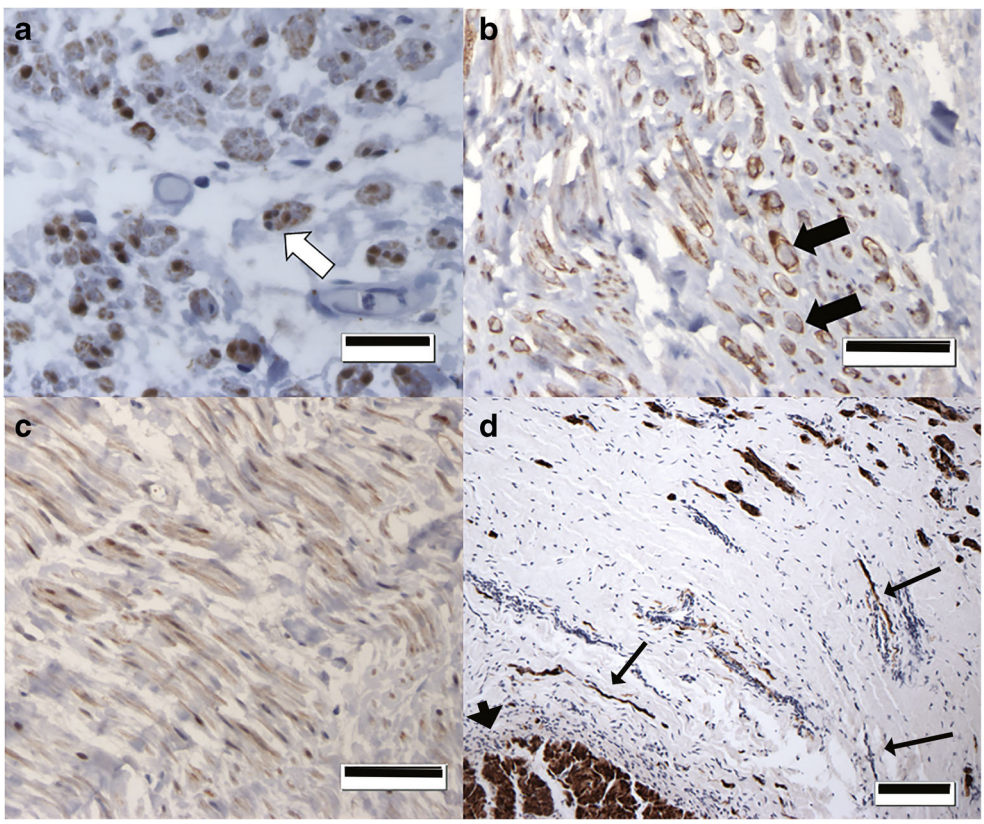


**Fig. 5** S100 IHC stains. S100 is a marker of neural crest-derived cells and is a marker of mature Schwann cells. **a** Schwann cells in neuroma samples (NIC, × 400; bar= 20 μm) appear within clusters (open arrow) similar to those of the NF200 staining axons (cf. Fig. 3a). **b** Interestingly, the Schwann cells in these clusters do not appear to form the typical lamellated myelin structures around large axons (black arrows) found in control specimens (× 200; bar= 50 μm). **c** A chronic avulsion specimen demonstrated the normal appearance of myelinating Schwann cells, but with reduced number or frequency within the specimen (× 200; bar= 50 μm). **d** S100-positive bundles (thin black arrows) were frequently seen to encircle intact fascicles (arrowhead) in NIC specimens (× 100; bar= 100 μm)

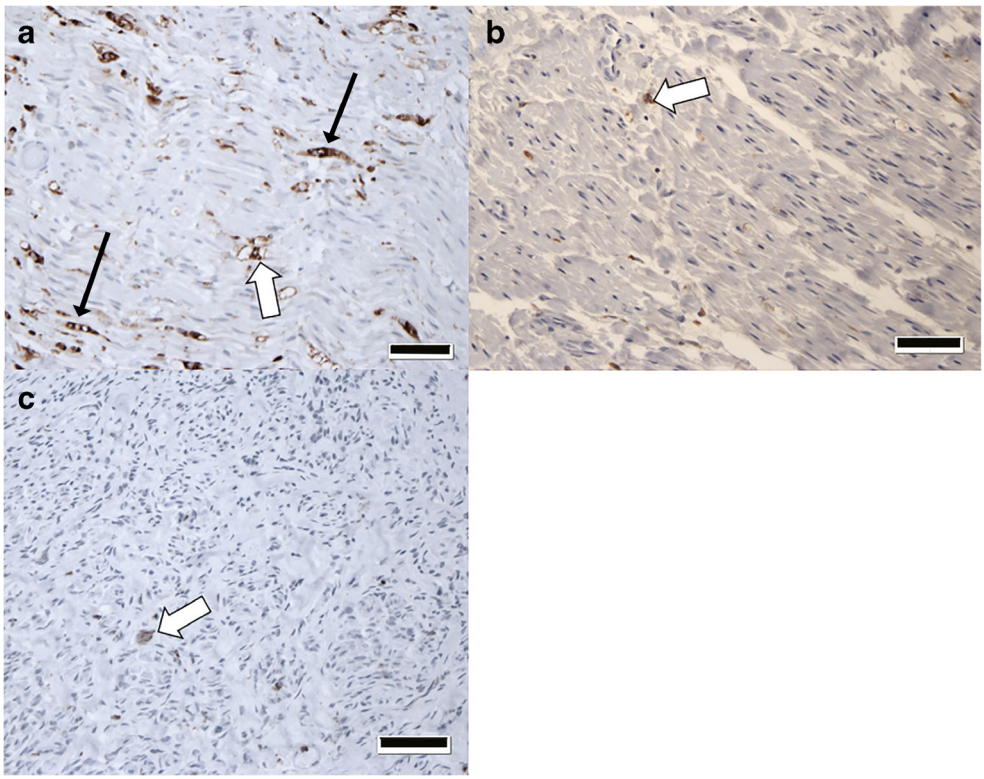


**Fig. 6** CD68 IHC stains. CD68 is a marker of lysosomes and is a canonical marker of activated macrophages. **a** An acute stump specimen obtained 6 days after injury (× 200; bar= 50 μm) demonstrated avid anti-CD68 staining with some cells demonstrating an appearance typical of the dendritic pattern of macrophages (open arrow) as well as cells with slender, fusiform shape (thin black arrows). **b** An avulsion specimen 2 days after injury (× 200; bar= 50 μm) demonstrated only a few dendritic-shaped CD68-positive cells (open arrow). **c** A chronic neuroma specimen (3 months after injury, × 200; bar= 50 μm) had rare CD68-positive cells (open arrow). Control specimens (not shown) had no CD68-positive cells

bundles encased in a GLUT1-rich sheath that is the hallmark of the perineurial blood–nerve barrier. These microfascicles contained Schwann cells without thick myelination, more consistent with the Remak bundle of small fibers. The neuromatous tissue had abundant capillaries within the dense collagenous stroma but lacked the arterioles found in larger fascicles. Large, activated phagocytes, as stained by the lysosomal protein CD68, were present during a narrow temporal window after injury; other macrophage subtypes, such as M2 macrophages, may be missed by CD68 staining. T-cells, however, were abundant in neuroma specimens, demonstrating a temporal pattern of clusters of T-cells in recent neuromas, e.g., around 3 months, and diffuse T-cell staining in neuromas over 12 months.

## Neuromas are a regenerative process

Neuromas display a highly consistent but disorganized structure that suggests a process of pathophysiologic healing. Avulsion specimens demonstrate no neuroma formation, despite the severity of injury. Thus, it seems that disruption of a fascicle of the nerve is required. Our clinical specimens demonstrate that neuroma formation occurs somewhere between 2 weeks and 3 months after injury. Jurecka et al. [20] noted that canonical neuroma pathology occurred at 3 weeks after transection in a mouse model.

The coordinating signaling that mediates neuroma formation has not been well established in animal experiments. It has been suggested that the fibroblastic reaction within the neuroma leads to excessive collagen deposition, which interferes with the blood supply to the growing axons, leading to ischemia and abnormal axonal function, as evident by the abnormal spontaneous electric discharges on electrophysiological studies [19, 35]. Additionally, fibroblasts from neuroma specimens appear to produce semaphorin 3a, which decreases neurite outgrowth in cell culture experiments [46].

## Perineurial encapsulated microfascicles are the pathology of regenerative neuromas

Nageotte [36] first identified bundles of regenerative axons within neuromas, work that was later verified and expanded by Masson [32] in the 1930s. Electron microscopic studies from the 1960s also identified small bundles in neuromas [20, 47]. The current IHC analysis demonstrates that the outer lumen of the double lumen is GLUT1 rich and is consistent with perineurium and the blood–nerve barrier [16, 34, 40, 48]. This consistent pattern suggests that perineurial cells participate in the fruitless regeneration of neuromas, either participating in the formation of the cellular bridge that is produced after nerve transection, later entering the bridge, or differentiating from other cells in the bridge.

Studies on transection models provide a clue. Cajal [41] and Denny-Brown's [10] experiments suggested that

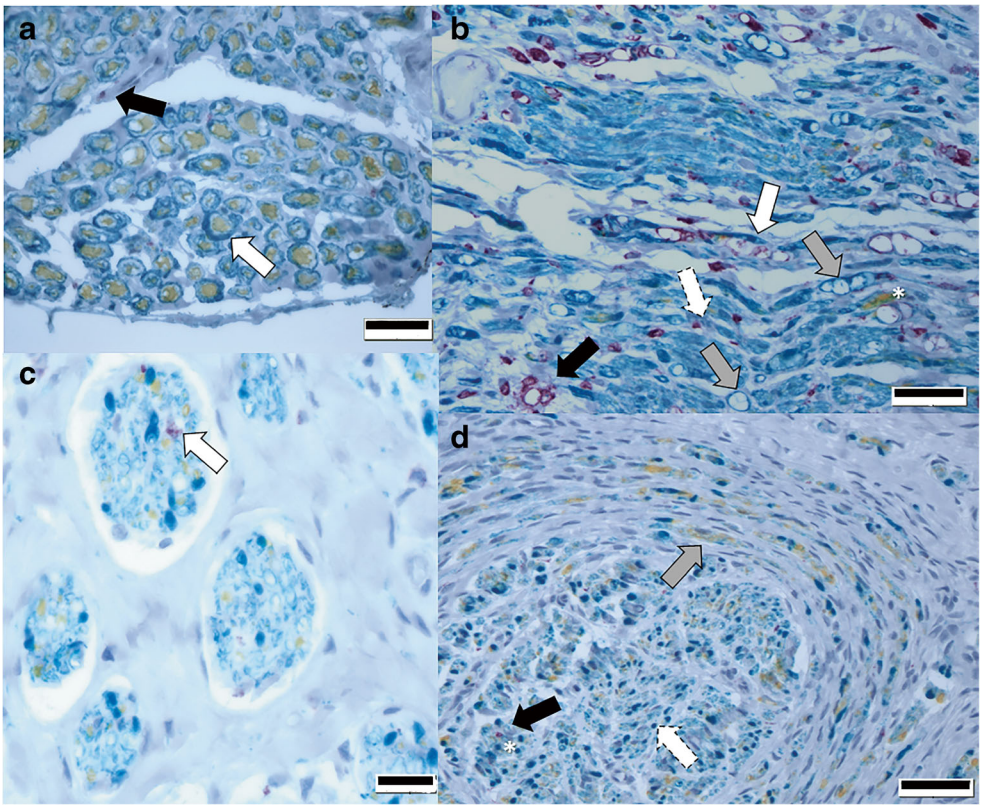


**Fig. 7** Triple IHC staining (anti-CD68 = purple; anti-NF200 = yellow; anti-S100 = teal; counterstain = hematoxylin/blue). Control specimens (**a**, × 600; bar= 10 μm) demonstrated typical fiber arrangement, with NF200 dense axons surrounded by S100-positive cells in a typical 1:1 myelinating morphology (open arrow). Faint CD68-positive cells are present, both in the endoneurium and in the vascular walls (black arrow). An acute stump specimen obtained 6 days after injury (**b**, × 200; bar= 50 μm) demonstrated avid anti-CD68 staining with large lipid-filled lysosomes (black arrow); however, not all lipid lysosomes had CD68 staining (gray arrows) and some CD68 lysosomes were in association with S100-positive cells (solid white arrow). As well, many CD68-positive cells were compact, suggestive of different macrophage subtypes (dashed arrow). Neurofilament was nearly absent, except in apparent degradation chambers. A chronic stump neuroma (**c**, 120 months, × 400; bar= 20 μm) demonstrated occasional CD68-positive cells (open arrow). S100 was much more abundant than neurofilament, without myelination pattern seen in the control specimen. A neuroma-in-continuity (**d**, 3 months, × 200; bar= 50 μm) with an intact fascicle depicted neurofilament with stippled S100 swirling around the intact fascicle (gray arrow). The intact fascicle has significantly less neurofilament than fascicles of control specimens as well as the surrounding neuroma (dashed arrow). CD68 staining was rare (black arrow)

perineurial and endoneurial fibroblasts were the first cells to produce the cellular bridge from the proximal stump, and Denny-Brown attributed the disorganization of a neuroma to the early proliferation of these fibroblasts. Contemporaries of the time provided evidence that Schwann cells were the initial cellular emigrants [17, 32, 36], which has provided a long controversy. Much of this conflict arose from the limitations of technique. Perineurial fibroblasts appear nearly identical to migrating Schwann cells under light microscopy, and similar even under electron microscopy (EM) [20]. EM studies suggested that perineurial fibroblasts were among the first cells at the defect of a proximal stump [20, 23, 44, 47, 50], a finding that has been corroborated by recent immunofluorescent studies showing migrating Schwann cells coordinated by fibroblasts [38]. Fibroblasts have been shown to be the cell of origin of perineurial cells [2]. In an elegant model, perineurial cells have been identified as bridging the gap of cut nerve fibers in time-lapse imaging of zebrafish, a process that preceded Schwann cell and axon outgrowth, suggesting that perineurial cells are the guidance channels for regenerating axons [29]. Corroboration of this work was provided by studies on the fetal development of peripheral nerves [26]. Thus, in neuromas, the elaborate reticular network of GLUT1 appears to be the hallmark of frustrated regeneration.

## Small fibers in Remak-type bundles

The axons in neuromas were predominantly small in diameter and were associated with non-myelinating-type Schwann cells, similar in appearance to Remak bundles. In neuroma specimens, S100-positive cells rarely demonstrated morphology such as is seen in myelinated fibers. A similar preponderance of small-diameter fibers was found in a rat model of neuroma [4], although the sample size used by the authors is too small to be confident of their results. Myelinated fibers in humans have an average axon diameter of 3.9 μm, as

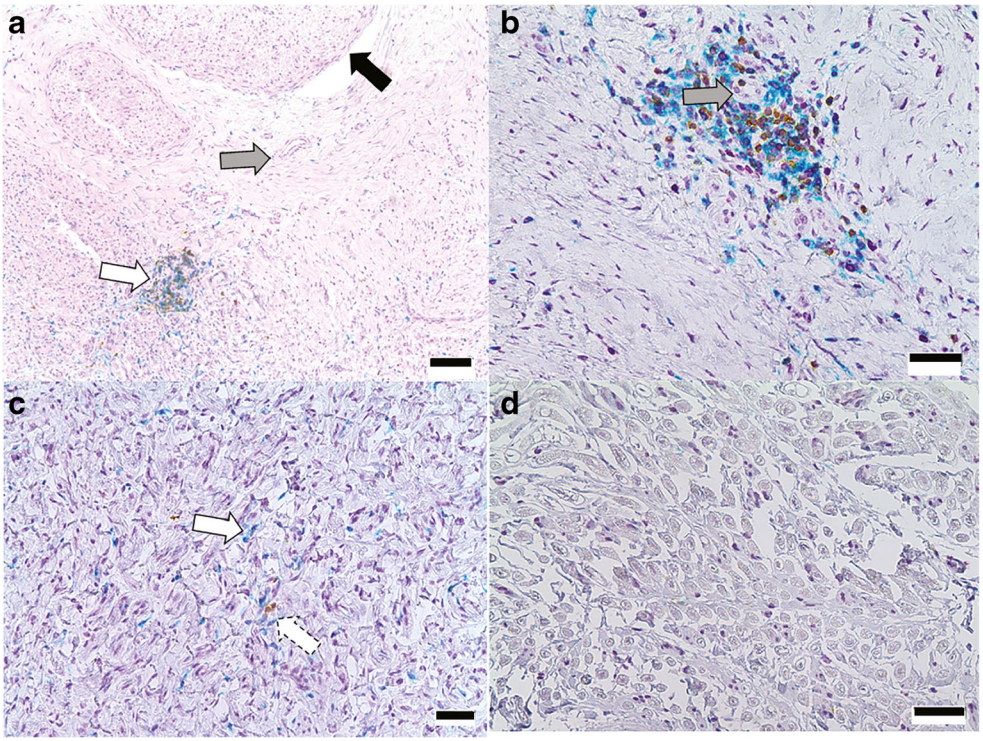


**Fig. 8** Triple IHC staining (anti-CD25 = purple; anti-CD3 = yellow; anti-CD4 = teal; counterstain = hematoxylin/blue). Neuroma-in-continuity specimen at 3 months after injury (**a**, × 100; bar= 100 μm) demonstrates a tight cluster of CD3+ and CD4+ cells in the neuromatous area (white arrow), without substantial evidence of T-cell staining in the intact fascicles (black arrow). Higher power view of a different cluster of T-cells in the same specimen (**b**, × 200; bar= 50 μm) demonstrates that the T-cell cluster appears coordinated around a vascular channel (gray arrow) but not all vascular channels have T-cell clusters (**a**, gray arrow). A chronic stump neuroma specimen at 12 months after transection (**c**, × 200; bar= 50 μm) demonstrates more diffuse CD4 (white arrow) and CD3 (dashed arrow) throughout the neuromatous area. Control specimens (**d**, × 200; bar= 50 μm) demonstrated little T-cell staining, except in epineurial vessel lumens (not shown here)

compared with average axon diameter in unmyelinated fibers of 0.8–1.2 μm [31, 33]. Automated counting of axon diameters from NF200 IHC staining revealed that > 73% of neuroma fibers were under 1.5 μm, compared with 44% in control specimens. More impressively, there was an absence of large axons in neuromas compared with normal controls: 5% of axons counted in NIC specimens were 2.6 μm or greater, as compared with 31% in control specimens. Many of the large and intermediate fibers in neuroma specimens were bundles too tight to be resolved by the algorithm and light microscopy.

Non-myelinating Schwann cells of Remak bundles support the survival of C-fiber sensory neurons, as demonstrated in a conditional knock-out mouse model [6]. However, the mechanism or pathology that ensures the existence of

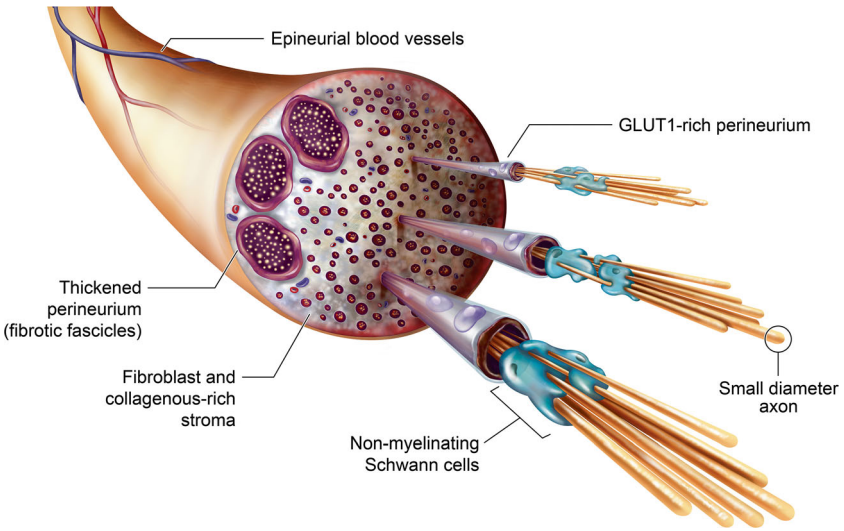


**Fig. 9** Artistic representation of the pathology of a human NIC. Intact fascicles demonstrate thickened perineurium. There is a dense fibrous stroma, which contains innumerable microfascicles that are hallmarked by a GLUT1-rich perineurium. Within the microfascicles, small-diameter axons are associated with mature Schwann cells without myelination, consistent with a Remak bundle. The neuromatous tissue had abundant capillaries within the dense fibrous tissue but lack arterioles of intact fascicles

predominantly small-diameter fibers in association with non-myelinating Schwann cells in a regenerative neuroma is uncertain and without sufficient experimental explanation.

## Significance of intact fascicles

Neuroma specimens frequently had apparently intact fascicles, which, when examined closely, demonstrate evident pathology compared with non-injured specimens, with myxoid edema, increased cellularity, thickening of the perineurium, and substantially reduced axon density. Virtually all NICs had one intact fascicle or more in the specimen, suggestive that the pathology of a NIC is the presence of a fascicular bridge. Intact fascicles were similarly abnormal whether they were injured months or years previously, retaining evidence of prior injury with fibrosis.

Previous stretching experiments in rabbit tibial nerves [14] demonstrated that fascicles ruptured individually and separately; as nerves underwent progressive stretch-mediated tearing, some fascicles appeared to possibly remain intact, while others tore away. These findings appear to be replicated in our NIC samples, with some intact-appearing fascicles. This is not unique to our specimens; specimens included by other authors demonstrate intact fascicles in neuroma histology—although not identified by the authors [3]. Thus, after a traction injury, whether the nerve undergoes complete rupture or forms a NIC appears to depend upon the presence of an intact fascicle. However, the presence of intact fascicles in one axial section of the NIC does not mean that this fascicle is continuous throughout the neuroma, as it could be injured proximal or distal to the intact-appearing axial section. Even if the fascicle were continuous, the presence of an intact fascicle does not mean reliable innervation. A recent study demonstrated the presence of spherical focal myelin deficits present throughout the NIC samples, which may be associated with dysfunction after NIC injuries [49].

## Macrophages

In acute nerve injuries, we identified abundant CD68 staining, of both apparent lipid-filled lysosomes as well as compact macrophages. The different-appearing macrophages likely represent identified subtypes of macrophages. Additionally, non-CD68 lysosomal bodies and CD68 lysosomes in association with S100-positive cells were seen. Schwann cells undergoing autophagy after Wallerian degeneration have been found to stain positively for CD68 [21] as well as numerous non-myeloid cells, like fibroblasts, endothelial cells, and carcinomas [13, 27]. Thus, although CD68 is a widely available clinical maker for macrophages, interpretation of CD68 staining in nerve injuries should be interpreted with caution because it may also stain Schwann cells or endoneurial fibroblasts.

We did not identify significant increases in CD68-positive cells in chronic neuromas, as compared with control nerves. The absence of CD68-positive cells in chronic neuromas from clinical specimens has been previously noted [49], but puzzlement was expressed by the authors on the absence of this staining. This is in contrast to work in a rodent neuroma model where ED1 is an antibody against the rodent homolog of human CD68 that found ED1-positive cells “in considerable numbers in the neuroma for at least one year” [12]. However, this model involved suture ligature as well as a cut nerve ending and thus is also a chronic compression lesion with a foreign body, not a simple neuroma. Thus, in contrast to the abundant experimental literature implying a role for activated macrophages in acute nerve regeneration [1, 5, 9, 11, 39], chronic neuromas do not appear to have an active innate immune inflammatory component.

## T-cells

Although we have not found prior reports of T-cells in human neuroma specimens, there are numerous reports on T-cell participation in animal experimental models of peripheral nerve injury. In particular, several groups have reported an association between T-cells and development of pain [25, 28], including the participation of Schwann cells as conditional antigen-presenting cells via expression of MHC-II, activation of T-cells, and promotion of pain behaviors [15]. The persistence of T-cells in human neuroma samples, especially because all of the chronic stump neuromas were resected for pain, also supports a potential role of chronic inflammation within the stump as a mechanism for pain. However, further studies would be required to support translation of the animal findings to human neuroma specimens.

## Limitations and considerations for future studies

There are numerous aspects of interpretation of clinical histology that limit universal application, including the sampling of representative images, site-specific protocols, image quantification, specimen number, and range of diagnoses, among others. Slicing of the neuroma was performed systematically through the largest diameter of the neuroma bulb. Our slicing did not evaluate the proximal portions of the neuroma, where additional insight might be gained. Furthermore, in small specimens, particularly the control nerves, achieving cross-section alignment is challenging, so some slices are partially oblique, which can confound interpretation of the course of the fibers within the neuroma. Although our clinical protocols are strengthened by use of positive controls, there is the

possibility of false negatives. Moreover, although we believe that clinical IHC provides the highest level of quality control and reproducibility, it lacks an easy ability for performing multiple concurrent immunostains, as is done with immunofluorescent imaging. As well, numerous additional antibodies could be used to study additional aspects of neuroma pathophysiology. For example, evaluation of non-myelinating Schwann cells should be studied with antibodies against myelin with costaining of S100. Antibodies against peripherin, a surface marker associated with smaller-diameter nerve fibers, may also yield insight into small fiber predominance in neuroma specimens. Alternatively, quantification of small fibers would optimally be performed using EM, but we did not prepare specimens for EM at the time of initial specimen processing and thus that option was lacking in our work. Western blot analysis of proteins or polymerase chain reaction analysis of gene products might provide additional insight. Lastly, inclusion of gene expression and automated counting of cellular composition may provide additional insight for future studies.

## Conclusion

Neuromas demonstrate a consistent pattern of pathology. Although neuromas appear chaotic on routine histologic staining, as compared with normal nerve specimens, there appear to be regular patterns of microarchitecture within the neuroma on IHC. Specifically, there was microfascicle formation with exquisitely complex perineurium, which is present in both NICs and stump neuromas. There is an absence of large, myelinated axons in neuromatous tissue. A feature consistent with NIC specimens was the presence of an intact-appearing fascicle; during traction injuries, the difference between NIC and complete severance may be the remnant of an intact fascicle. Lastly, neuromas harbored substantial T-cell populations for long after injury, which may relate to chronic pain. It appears that the neuroma is a specific pathophysiologic reaction, which deserves greater exploration and mechanistic evaluation.

## Compliance with ethical standards

**Conflict of interest** The authors declare that they have no conflict of interest.

**Research involving human participants or animals** All human and animal studies have been approved by the appropriate ethics committee and have therefore been performed in accordance with the ethical standards laid down in the 1964 Declaration of Helsinki and its later amendments.

**Informed consent** The study was approved by the institutional review board at the University of Utah with wavier of informed consent from the patients involved in the study.

## References


1. Brown-Séquard C (1881) On certain physiological effects of stretching of the sciatic nerve. Lancet 117:206
2. Bunge M, Wood P, Tynan L, Bates M, Sanes (1989) Perineurium originates from fibroblasts: demonstration in vitro with a retroviral marker. Science 243:229–231. https://doi.org/10.1126/science.2492115
3. Burks SS, Cajigas I, Jose J, Levi AD (2017) Intraoperative imaging in traumatic peripheral nerve lesions: correlating histologic cross-sections with high-resolution ultrasound. Oper Neurosurg (Hagerstown) 13:196–203. https://doi.org/10.1093/ons/opw016
4. Carlton SM, Dougherty PM, Pover CM, Coggeshall RE (1991) Neuroma formation and numbers of axons in a rat model of experimental peripheral neuropathy. Neurosci Lett 131:88–92. https://doi.org/10.1016/0304-3940(91)90343-R
5. Cattin AL, Burden JJ, Van Emmenis L, Mackenzie FE, Hoving JJ, Garcia Calavia N, Guo Y, McLaughlin M, Rosenberg LH, Quereda V, Jamecna D, Napoli I, Parrinello S, Enver T, Ruhrberg C, Lloyd AC (2015) Macrophage-induced blood vessels guide Schwann cell-mediated regeneration of peripheral nerves. Cell 162:1127–1139. https://doi.org/10.1016/j.cell.2015.07.021
6. Chen S, Rio C, Ji R-R, Dikkes P, Coggeshall RE, Woolf CJ, Corfas G (2003) Disruption of ErbB receptor signaling in adult non-myelinating Schwann cells causes progressive sensory loss. Nat Neurosci 6:1186. https://doi.org/10.1038/nn1139
7. Chen ZL, Yu WM, Strickland S (2007) Peripheral regeneration. Annu Rev Neurosci 30:209–233. https://doi.org/10.1146/annurev.neuro.30.051606.094337
8. Chiono V, Tonda-Turo C, Ciardelli G (2009) Chapter 9: artificial scaffolds for peripheral nerve reconstruction. Int Rev Neurobiol 87:173–198. https://doi.org/10.1016/S0074-7742(09)87009-8
9. Dailey AT, Avellino AM, Benthem L, Silver J, Kliot M (1998) Complement depletion reduces macrophage infiltration and activation during Wallerian degeneration and axonal regeneration. J Neurosci 18:6713–6722
10. Denny-Brown D (1946) Importance of neural fibroblasts in the regeneration of nerve. Arch Neurol Psychiatr 55:171–215
11. Fregnan F, Muratori L, Simoes AR, Giacobini-Robecchi MG, Raimondo S (2012) Role of inflammatory cytokines in peripheral nerve injury. Neural Regen Res 7:2259–2266. https://doi.org/10.3969/j.issn.1673-5374.2012.29.003
12. Frisen J, Risling M, Fried K (1993) Distribution and axonal relations of macrophages in a neuroma. Neuroscience 55:1003–1013
13. Gottfried E, Kunz-Schughart LA, Weber A, Rehli M, Peuker A, Muller A, Kastenberger M, Brockhoff G, Andreesen R, Kreutz M (2008) Expression of CD68 in non-myeloid cell types. Scand J Immunol 67:453–463. https://doi.org/10.1111/j.1365-3083.2008.02091.x
14. Haftek J (1970) Stretch injury of peripheral nerve. Acute effects of stretching on rabbit nerve. J Bone Joint Surg (Br) 52:354–365
15. Hartlehnert M, Derksen A, Hagenacker T, Kindermann D, Schafers M, Pawlak M, Kieseier BC, Meyer Zu Horste G (2017) Schwann

cells promote post-traumatic nerve inflammation and neuropathic pain through MHC class II. Sci Rep 7:12518. https://doi.org/10.1038/s41598-017-12744-2
16. Hirose T, Tani T, Shimada T, Ishizawa K, Shimada S, Sano T (2003) Immunohistochemical demonstration of EMA/Glut1-positive perineurial cells and CD34-positive fibroblastic cells in peripheral nerve sheath tumors. Mod Pathol 16:293–298. https://doi.org/10.1097/01.MP.0000062654.83617.B7
17. Holmes W, Young JZ (1942) Nerve regeneration after immediate and delayed suture. J Anat 77(63–96):10
18. Holness CL, Simmons DL (1993) Molecular cloning of CD68, a human macrophage marker related to lysosomal glycoproteins. Blood 81:1607–1613
19. Jung J, Hahn P, Choi B, Mozaffar T, Gupta R (2014) Early surgical decompression restores neurovascular blood flow and ischemic parameters in an in vivo animal model of nerve compression injury. J Bone Joint Surg Am 96:897–906. https://doi.org/10.2106/JBJS.M.01116
20. Jurecka W, Ammerer HP, Lassmann H (1975) Regeneration of a transected peripheral nerve. An autoradiographic and electron microscopic study. Acta Neuropathol 32:299–312
21. Kaiserling E, Xiao JC, Ruck P, Horny HP (1993) Aberrant expression of macrophage-associated antigens (CD68 and Ki-M1P) by Schwann cells in reactive and neoplastic neural tissue. Light- and electron-microscopic findings. Mod Pathol 6:463–468
22. Karsy M, Palmer CA, Mahan MA (2018) Pathologic remodeling of endoneurial tubules in human neuromas. Cureus 10:e2087. https://doi.org/10.7759/cureus.2087
23. Katenkamp D, Stiller D (1978) Ultrastructure of perineurial cells during peripheral nerve regeneration. Electron microscopical investigations on the so-called amputation neuroma. Exp Pathol (Jena) 16:5–15
24. Kingham PJ, Kalbermatten DF, Mahay D, Armstrong SJ, Wiberg M, Terenghi G (2007) Adipose-derived stem cells differentiate into a Schwann cell phenotype and promote neurite outgrowth in vitro. Exp Neurol 207:267–274
25. Kleinschnitz C, Hofstetter HH, Meuth SG, Braeuninger S, Sommer C, Stoll G (2006) T cell infiltration after chronic constriction injury of mouse sciatic nerve is associated with interleukin-17 expression. Exp Neurol 200:480–485. https://doi.org/10.1016/j.expneurol.2006.03.014
26. Kucenas S, Takada N, Park H-C, Woodruff E, Broadie K, Appel B (2008) CNS-derived glia ensheath peripheral nerves and mediate motor root development. Nat Neurosci 11:143. https://doi.org/10.1038/nn2025 https://www.nature.com/articles/nn2025#supplementary-information
27. Kunz-Schughart LA, Weber A, Rehli M, Gottfried E, Brockhoff G, Krause SW, Andreesen R, Kreutz M (2003) The "classical" macrophage marker CD68 is strongly expressed in primary human fibroblasts. Verh Dtsch Ges Pathol 87:215–223
28. Lees JG, Duffy SS, Perera CJ, Moalem-Taylor G (2015) Depletion of Foxp3+ regulatory T cells increases severity of mechanical allodynia and significantly alters systemic cytokine levels following peripheral nerve injury. Cytokine 71:207–214. https://doi.org/10.1016/j.cyto.2014.10.028
29. Lewis GM, Kucenas S (2014) Perineurial glia are essential for motor axon regrowth following nerve injury. J Neurosci 34:12762–12777. https://doi.org/10.1523/JNEUROSCI.1906-14.2014
30. Mahan MA (2018) Nerve stretching: a history of tension. J Neurosurg. https://doi.org/10.3171/2018.8.JNS173181
31. Malik RA, Tesfaye S, Newrick PG, Walker D, Rajbhandari SM, Siddique I, Sharma AK, Boulton AJM, King RHM, Thomas PK, Ward JD (2005) Sural nerve pathology in diabetic patients with minimal but progressive neuropathy. Diabetologia 48:578–585. https://doi.org/10.1007/s00125-004-1663-5
32. Masson P (1932) Experimental and spontaneous schwannomas (peripheral gliomas): I. Experimental schwannomas. Am J Pathol 8(367–388):361
33. Mohseni S, Badii M, Kylhammar A, Thomsen NOB, Eriksson KF, Malik RA, Rosen I, Dahlin LB (2017) Longitudinal study of neuropathy, microangiopathy, and autophagy in sural nerve: implications for diabetic neuropathy. Brain Behav 7:e00763. https://doi.org/10.1002/brb3.763
34. Muona P, Sollberg S, Peltonen J, Uitto J (1992) Glucose transporters of rat peripheral nerve. Differential expression of GLUT1 gene by Schwann cells and perineural cells in vivo and in vitro. Diabetes 41:1587–1596
35. Myers RR, Heckman HM, Galbraith JA, Powell HC (1991) Subperineurial demyelination associated with reduced nerve blood flow and oxygen tension after epineurial vascular stripping. Lab Investig 65:41–50
36. Nageotte J (1932) Sheaths of the peripheral nerves. Nerve degeneration and regeneration. In: Penfield W (ed) Cytology and cellular pathology of the nervous system. Hoeber, New York
37. Odier L (1811) Manuel de Medecine Pratique, 2nd ed. J. Paschoud, Paris
38. Parrinello S, Napoli I, Ribeiro S, Digby PW, Fedorova M, Parkinson DB, Doddrell RD, Nakayama M, Adams RH, Lloyd AC (2010) EphB signaling directs peripheral nerve regeneration through Sox2-dependent Schwann cell sorting. Cell 143:145–155
39. Perry V, Brown M, Gordon S (1987) The macrophage response to central and peripheral nerve injury. A possible role for macrophages in regeneration. J Exp Med 165:1218–1223
40. Pina AR, Martinez MM, de Almeida OP (2015) Glut-1, best immunohistochemical marker for perineurial cells. Head Neck Pathol 9:104–106. https://doi.org/10.1007/s12105-014-0544-6
41. Ramon y Cajal S, DeFelipe J, Jones E (eds) (1991) Cajal's degeneration and regeneration of the nervous system. Oxford University Press, Oxford
42. Richard L, Topilko P, Magy L, Decouvelaere A-V, Charnay P, Funalot B, Vallat J-M (2012) Endoneurial fibroblast-like cells. J Neuropathol Exp Neurol 71:938–947
43. Schlaepfer WW (1987) Presidential address: neurofilaments: structure, metabolism and implications in disease. J Neuropathol Exp Neurol 46:117–129. https://doi.org/10.1097/00005072-198703000-00001
44. Schroder JM, May R, Weis J (1993) Perineurial cells are the first to traverse gaps of peripheral nerves in silicone tubes. Clin Neurol Neurosurg 95(Suppl):S78–S83
45. Sunderland S (1951) A classification of peripheral nerve injuries producing loss of function. Brain 74:491–516
46. Tannemaat MR, Korecka J, Ehlert EME, Mason MRJ, van Duinen SG, Boer GJ, Malessy MJA, Verhaagen J (2007) Human neuroma contains increased levels of semaphorin 3A, which surrounds nerve fibers and reduces neurite extension in vitro. J Neurosci 27:14260–14264. https://doi.org/10.1523/jneurosci.4571-07.2007
47. Thomas PK, Jones DG (1967) The cellular response to nerve injury. II Regeneration of the perineurium after nerve section. J Anat 101:45–55
48. Tserentsoodol N, Shin BC, Koyama H, Suzuki T, Takata K (1999) Immunolocalization of tight junction proteins, occludin and ZO-1, and glucose transporter GLUT1 in the cells of the blood-nerve barrier. Arch Histol Cytol 62:459–469

49. van Vliet AC, Tannemaat MR, van Duinen SG, Verhaagen J, Malessy MJ, De Winter F (2015) Human neuroma-in-continuity contains focal deficits in myelination. J Neuropathol Exp Neurol 74:901–911. https://doi.org/10.1097/nen.0000000000000229
50. Weis J, May R, Schroder JM (1994) Fine structural and immunohistochemical identification of perineurial cells connecting proximal and distal stumps of transected peripheral nerves at early stages of regeneration in silicone tubes. Acta Neuropathol 88:159–165
51. Wood W (1829) Observations on neuromas. With cases and histories of the disease. Trans Med Chir Soc Edinb 3:367–434



**Comments**

An ambitious and interesting article that examines the histopathology of various types of human neuromas (stump, in continuity, and avulsion types) as compared to normal control nerve specimens using standard as well as immunohistochemical tissue staining techniques. Despite some attempt at quantification (e.g., axon diameters shown in Fig. 3c), most of the observations made are qualitative in nature. Many of the observations are reasonable and supported by other studies both in humans and animals. The authors do comment on the surprising finding of little staining of macrophages using CD68 in most of their tissue specimens and provide some possible explanations. In future studies, it would be interesting to stain their tissue specimens for proteoglycans which have been shown to play a role in influencing axonal regeneration following nerve injury.

Michel Kliot
CA, USA